February 4, 2002
LAPP-EXP-2002-02
AMS Note 2002-01-03

Study of the photomuliplier R7600-00-M4 for the purpose of the electromagnetic calorimeter in the AMS-02 experiment.

Roman Kossakowski, Jean Charles Audemer, Jean Marc Dubois, Denis Fougeron, Richard Hermel, Rico Sottile, Jean Pierre Vialle

LAPP - Laboratoire d'Annecy le Vieux de Physique des Particules
BP 110
F-74941 Annecy –le-Vieux Cedex

Abstract
The properties of the 4-channels photomultiplier R7600-00-M4 from Hamamatsu were extensively studied for use in the AMS-02 electromagnetic calorimeter. A scan of the photocathode with a precision in position better than 0.1 mm was performed in order to measure the position dependence of the sensitivity and of the cross talk between pixels. The influence of the magnetic field applied in X, Y and Z directions was measured. The dynamic range of the photomultiplier was measured and optimized by the appropriate choice of the high voltage divider and of the value of the high voltage.

Introduction
The AMS-02 [1] experiment aims at measuring the cosmic ray spectra in the range of energy from GeV to TeV during three years on the International Space Station ISS. The experimental set-up consists in a superconducting magnet, a silicon tracker and a number of additional detectors, designed to measure the energy and to identify the nature of cosmic ray. These detectors are: the transition radiation detector (TRD), the time of flight (TOF) which also provides a standard AMS trigger, the ring imaging Cerenkov counter (RICH) and the electromagnetic calorimeter (ECAL). The detailed description of the AMS-02 detector can be found in [2].

The electromagnetic calorimeter, which is constructed by Annecy (France), Beijing (China) and Pisa (Italy) collaboration, will be a major instrument to identify electrons, positrons and γ-rays and to measure their energy in the high energy part of the spectrum. The ECAL is an imaging calorimeter consisting of 9 modules made of layers of Lead and scintillating fibers (figure 1). Each module has 648x648 mm^2 section and 18 mm depth, which corresponds to ~1.8 radiation lengths. In two successive modules the fibers are rotated by 90° and follow or X or Y direction. The fibers of a module are read only at one end by photmultipliers R7600-00-M4 from Hamamatsu [3], placed alternatively on each side. One photomultiplier consists of 4 « independent » pixels. In this way the elementary cell of the calorimeter has the dimension of 648x9mm^2 (or 9x648mm^2) in X-Y directions and 9mm in Z direction. It corresponds roughly to ~1 Molière radius for the transverse dimension of the electromagnetic

shower and to ~1 radiation length in the longitudinal direction. A particle impinging vertically on the ECAL crosses ~16.5 radiation lengths and the longitudinal profile of the electromagnetic shower is sampled by 18 independent measurements (figure 1).

The major challenge for the photomultiplier and for its front-end electronics is related to the very large dynamic range of light pulses created in optical fibers by cosmic rays. The signal in the photomultiplier ranges from a few photoelectrons for minimum ionizing particles (MIP's) to about 10^5 photoelectrons for electromagnetic showers corresponding to very high energy particles (for instance an electron of 1 TeV energy) [4]. Another challenge comes from the rather strong residual magnetic field coming from the superconducting magnet. At the position of the ECAL, the magnetic field ranges up to 300 Gauss and its value and direction changes from one photomultiplier position to another one. The weight budget allowed for the detector and the space available between photomultipliers are very limited, this implies a fine optimization between the response of the photomultipliers on the magnetic field and the design of the magnetic shielding.

In this paper we present the results of the measurements of several properties of the R7600-00-M4 photomultiplier. The photocathode sensitivity of the PMT and the cross talk between pixels were scanned with a precision of the order of 0.1mm, which allowed the optimization of dimensions of the light collecting cones: these results are described in the first section. In the second section are presented the measurements of the influence of the magnetic field applied in X, Y and Z directions on the performances of the photomultiplier. Finally, the third section describes the evolution of the dynamic range of the photomultiplier with applied high voltage for several high voltage dividers.

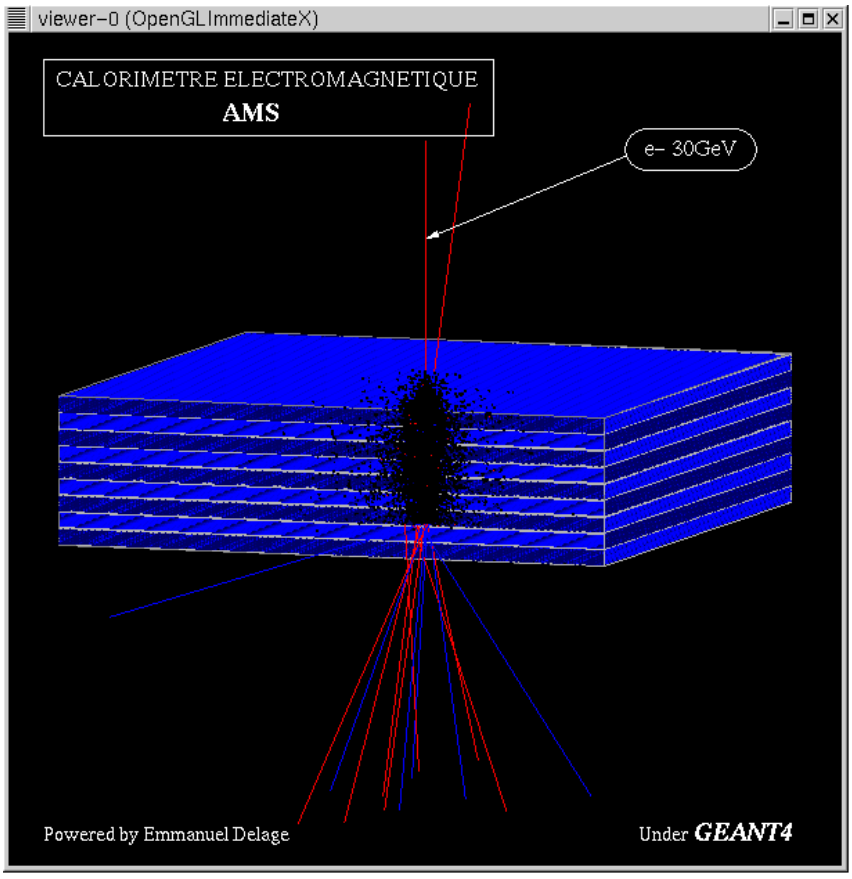

Figure 1. Schematic view of the electromagnetic calorimeter for AMS02 experiment.

1. Position dependent photocathode sensitivity and cross talk between pixels.

For the scanning of the photocathode, the PMT was fixed on an X-Y table, moving in front of the LED, whose light was collimated by a 9mm long and 0.5mm diameter black tube (figures 1 and 2).

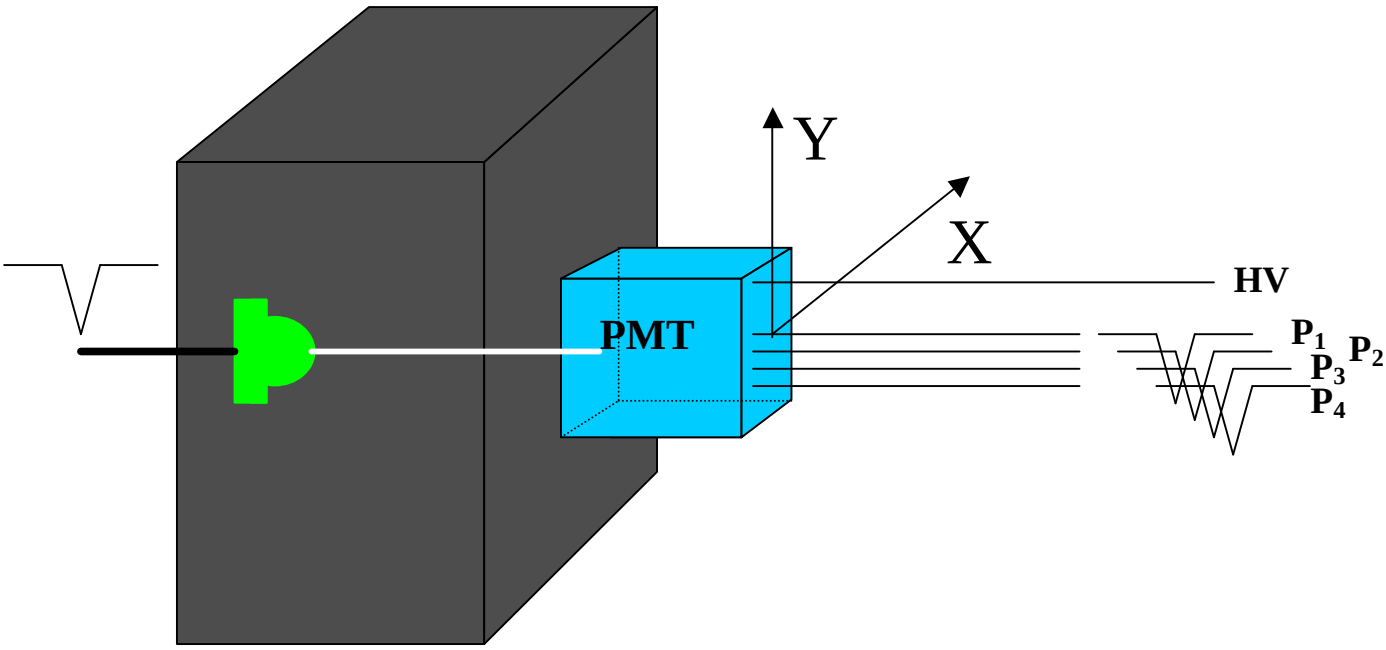

Figure 1. The PMT is mounted on the X-Y table. The light pulse from LED is collimated by the 9mm long and 0.5mm diameter black tube. Signals from 4 PMT pixels are collected by the acquisition system.

Figure 2. Two views of the experimental set-up. The left one shows the PMT mounted on the X-Y support. Four signal cables (white) and one HV supply cable (red) can be observed on the PMT HV divider. The gray cable supplies the LED light source. On the right: The set-up covered by black cloth for light tightness is ready for acquisition. The screws for X and Y motion can be observed.

A typical scanning is shown in figure 3: the LED light source is moved along X (or Y) axis for a fixed Y (or X) position. For each X (or Y) position the response of 4 PMT pixels (P_1 to P_4) is collected for 10000 light pulses. The average signal (ADC position after pedestal subtraction) and the dispersion (RMS) are then calculated for each pixel.

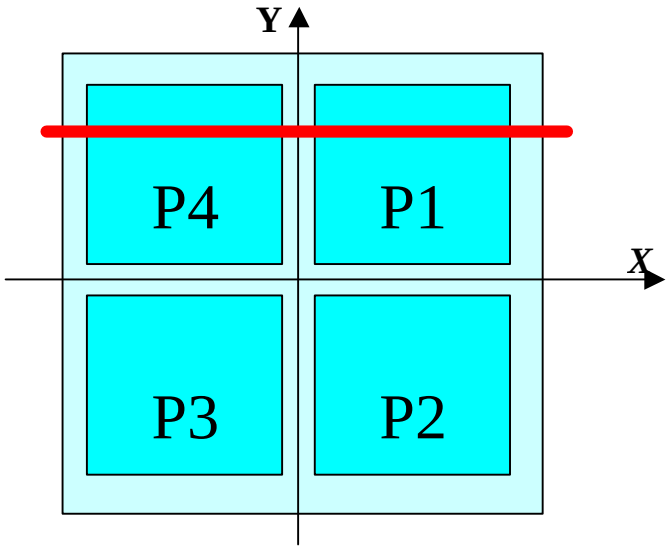

Figure 3. An example of the scan of the PMT photocathode at a fixed Y position (Y = + 6mm in this case – red line). One expects a non-zero signal for P_4 pixel for negative X values and a non zero-signal for P_1 for positive X values.

Signals collected for Y = +6mm scanning are shown on the figure 4. One can observe a non-zero signal for P_4 pixel for –8mm < X < 0 and a non-zero signal for P_1 pixel for 0 < X < +8mm. The signal uniformity is of about ± 20%. At the frontier between pixels a thin area of about 0.5 mm where both pixels are active can be observed. The observed periodical structure of signals can be explained by the internal structure of the photomultiplier, made of parallel strips along Y-axis with 1 mm pitch (fig 5).

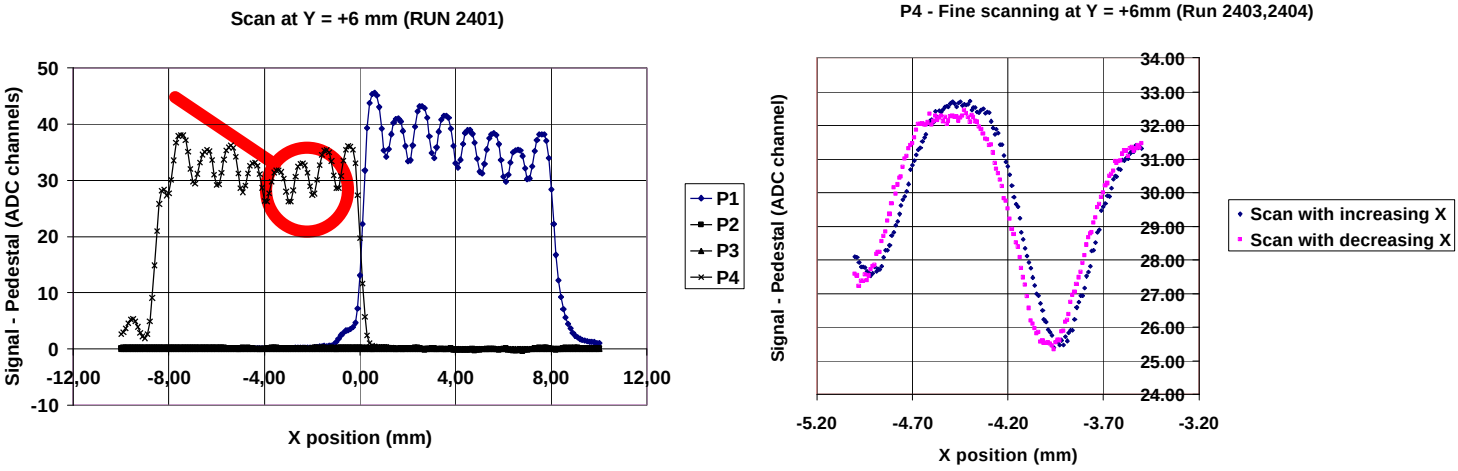

Figure 4. Left: signals collected for 4 pixels (P_1 to P_4) of the photomultiplier as function of the light impact position in X direction. Right: Detail of the signal collected for P4 (zoom from left figure). The shift of the curve measured for increasing X values with respect to the one measured for decreasing X values allows to set the mechanical precision of the measurement of X to be 0.05 mm.

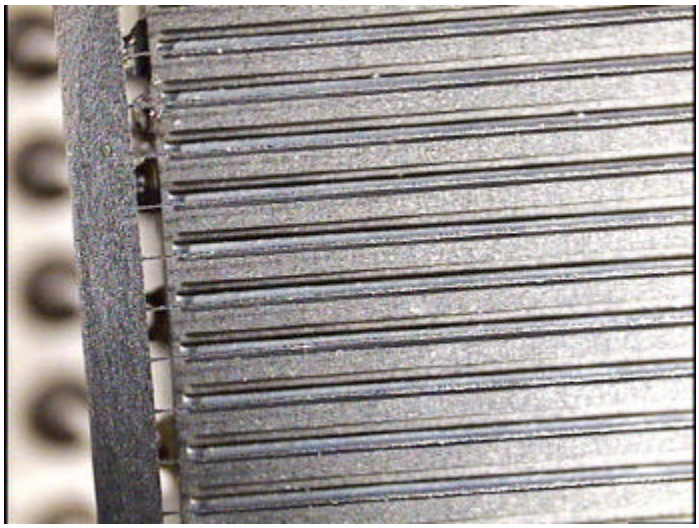

Figure 5. Blow up of the internal structure of the photomultiplier. One can observe the parallel grids structure.

From the amplitude A and the RMS of the signal s one can calculate the gain G and the number of collected photoelectrons N_{pe} following the formulas:

$$G = a\,s^2 / eA \qquad N_{pe} = A^2 / s^2$$

where a = 0.25 10^{-12} Coulomb/channel (ADC calibration) and $\boldsymbol{e}$ = 1.6 10^{-19} Coulomb (charge of one electron). The evolution of N_{pe} and G for P_1 and P_4 are shown in figure 6 (the signal collected is shown for comparison). It can be observed that the 1mm periodic structure of the signal is due to the fluctuation in N_{pe}, and the global evolution of the signal is related to the gain G.

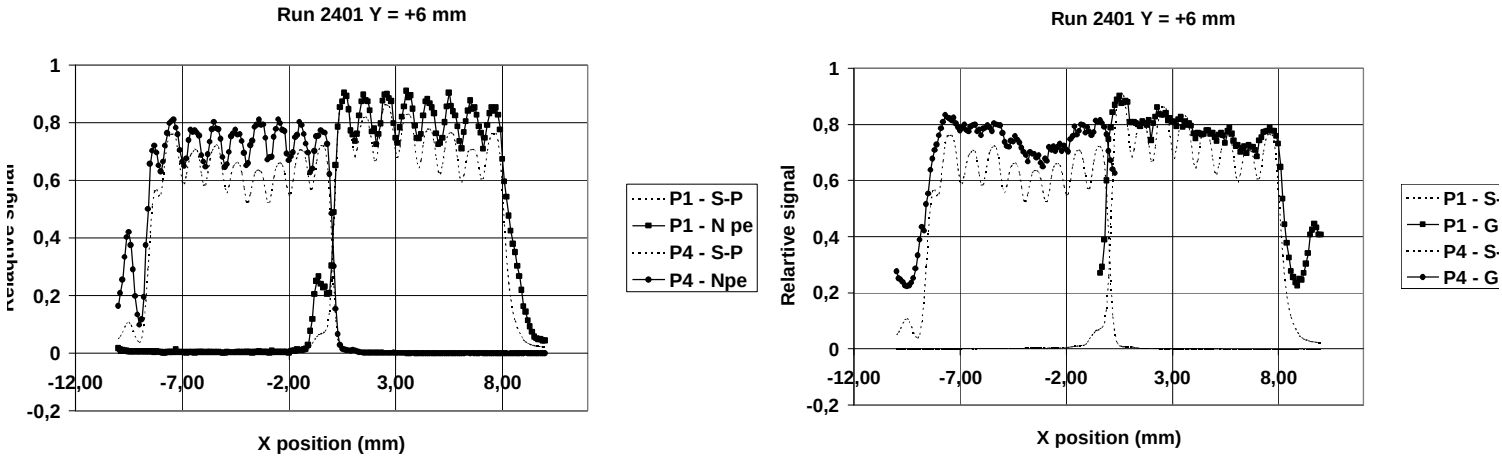

Figure 6. The dependence of the relative number of photoelectrons (left) and of the relative gain (right) with the position of the light source. The evolution of the signal collected is shown on both figures for comparison.

The results of the scanning at fixed X=+2mm position are presented in figures 7 for P_1 and P_2. As expected, this scanning along Y axis shows no oscillating structure, the signal uniformity is of about ±20% for the Y values limited by ±8mm on the outer side and ±0.5mm in the inner side.

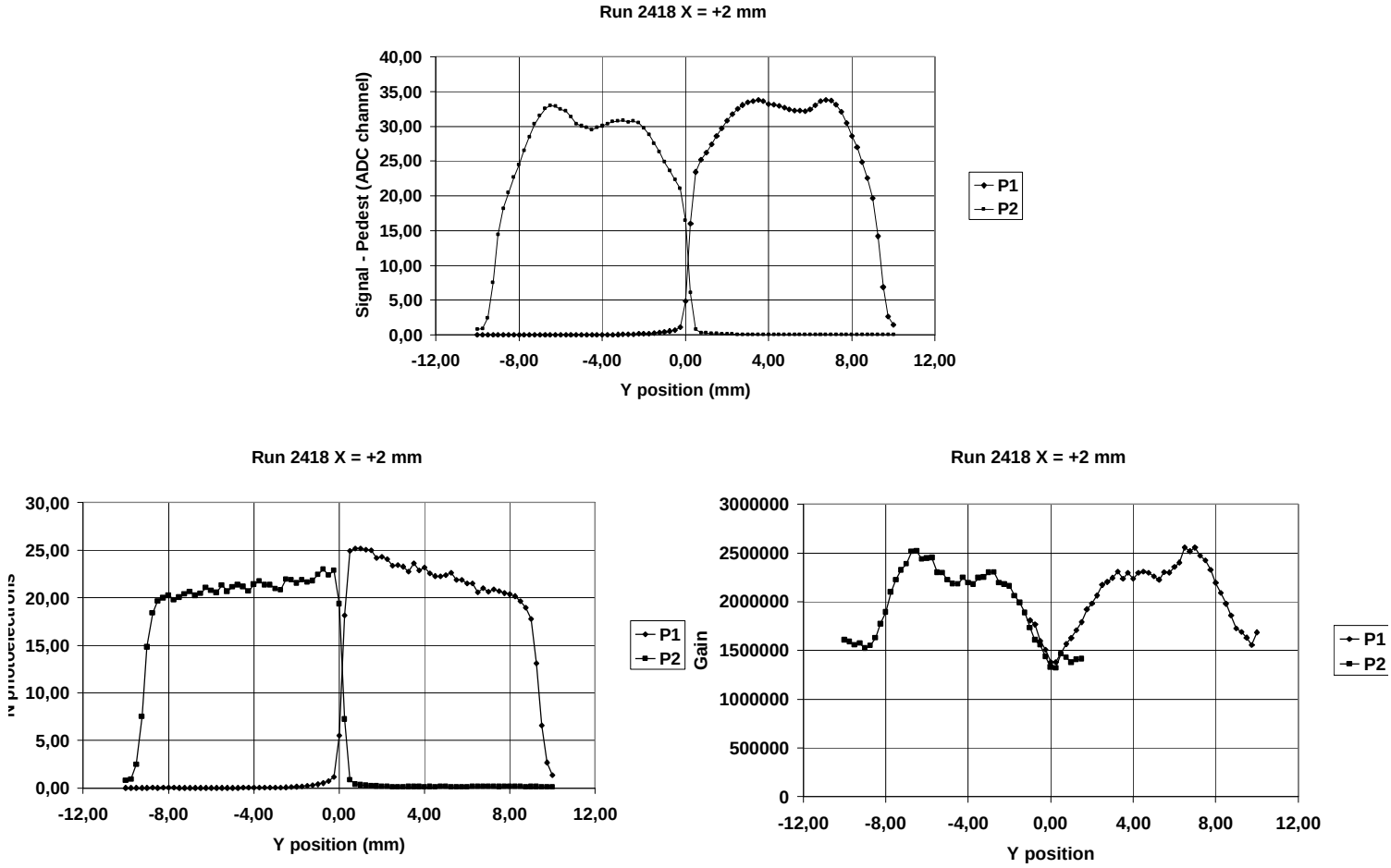

Figure 7. Same as figures 5 and 6, but for the scanning along Y-axis at X = +2mm.

The scanning was performed in 11 different positions, which are summarized in figure 8. The range of the area, which corresponds to the signal uniformity of 70% and the cross talk between channels less than 10% is indicated by the red line for each scanning.

Finally, regions in blue on the figure 8 (ranging from ±0.5mm to ±7.0mm in both X and Y directions) indicate the size of pixels adopted for the light collectors designed for the calorimeter (these light guides are necessary to transport light coming out from the calorimeter to the photomultiplier, moved back inside the magnetic shielding tube).

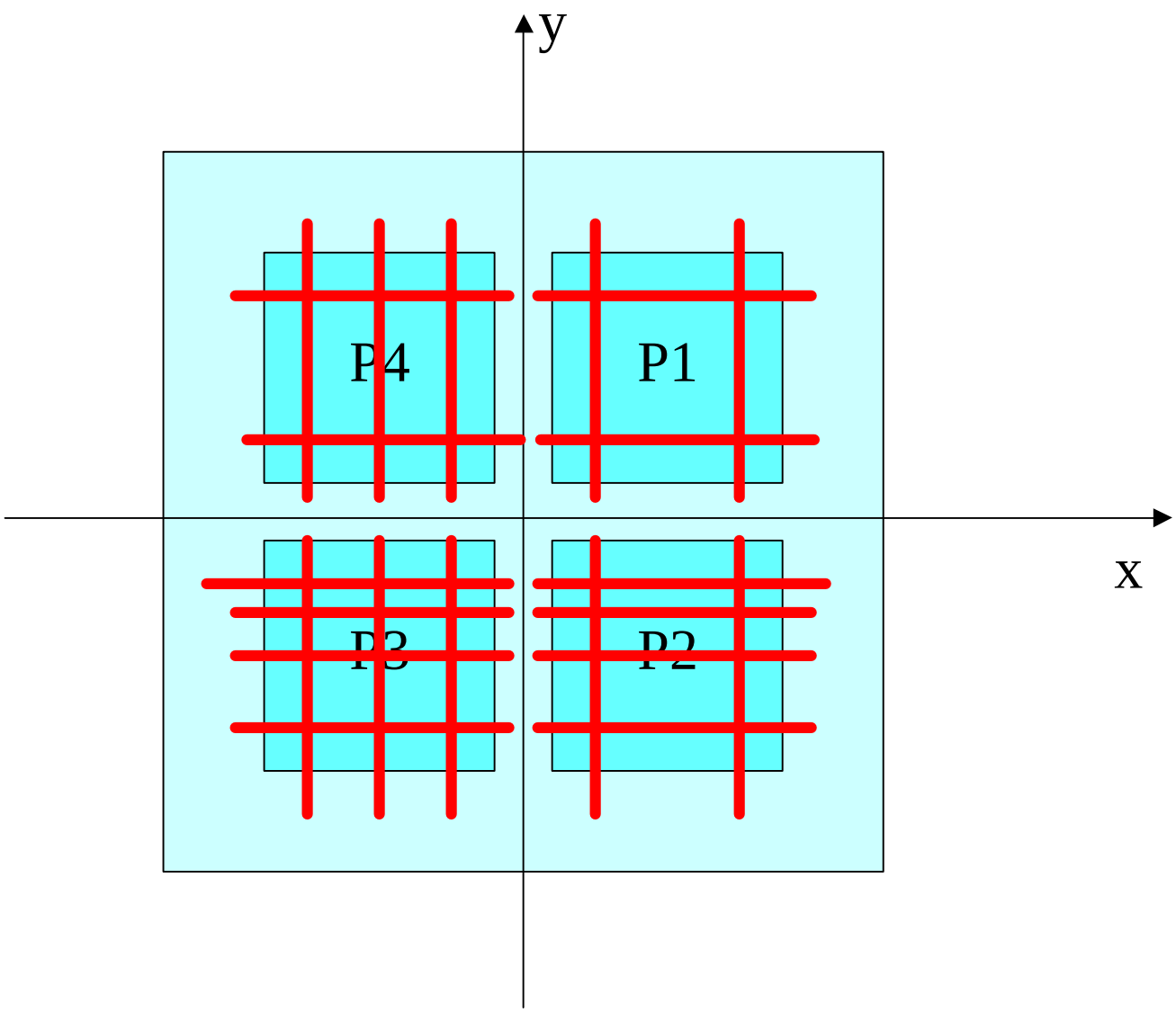

Figure 8. The range of the photocathode surface corresponding to a signal uniformity better than 70% and a cross talk between pixels smaller than 10%.

2. Magnetic field effect on the response of the photomultiplier

As it was mentioned in the introduction, the magnetic field from the AMS-02 superconducting magnet is of the order of 200 – 300 Gauss in the region where the calorimeter is placed. The limit of the weight and the small space available between photmultipliers impose to optimize the thickness of the materials used for magnetic shielding. The detailed calculations corresponding to this optimization can be found in [5], we present in this section the measurements of the sensitivity of the photomultiplier to the magnetic field. The photomultiplier was put inside of the magnetic solenoid (figure 9), which produced the magnetic field in the range of ±500 Gauss. The system of 4 LED's illuminated separately 4 pixels of the photomultiplier. The signal was then measured for 3 different directions of the magnetic field.

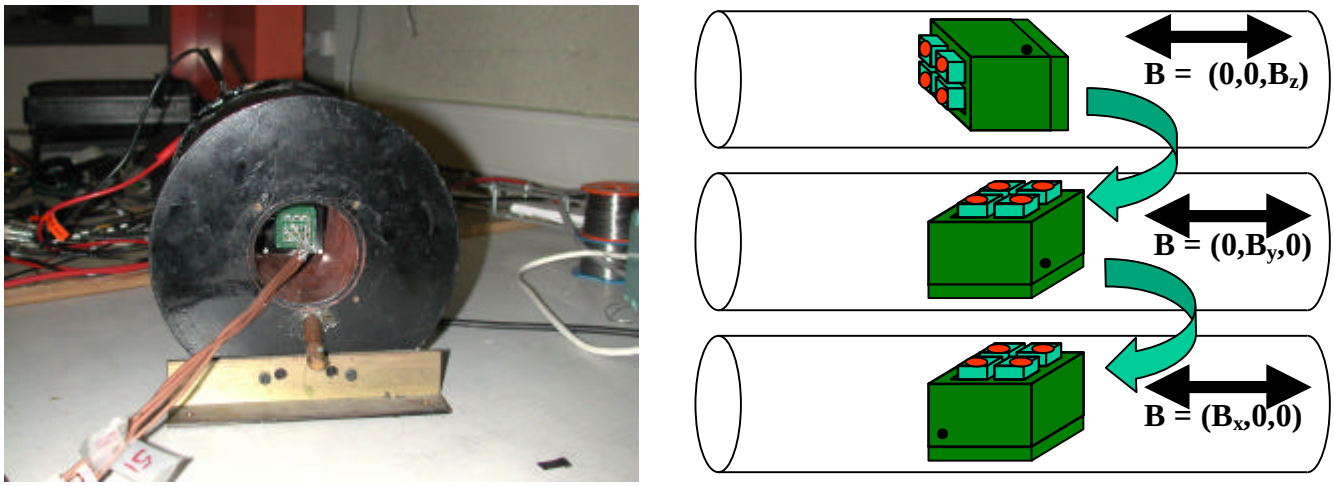

Figure 9. The photmultiplier inside the solenoid (B from 0 to ±500 Gauss). The X, Y and Z directions of the magnetic field were obtained by the rotation of the PMT inside the solenoid.

In the volume of the PMT, the uniformity of the magnetic field produced by the solenoid was better than 0.5%. The results of the measurements are given in figures 10, 11 and 12 for $\mathbf{B_X}$, $\mathbf{B_Y}$ and $\mathbf{B_Z}$ components respectively. One can observe the significant reduction of the signal for $\mathbf{B_X}$ and $\mathbf{B_Z}$ components (as expected from the Hamamatsu data sheets for the equivalent, single pixel photomultiplier) and much smaller influence of the magnetic field applied in **Y** direction. In Y and Z directions, the measurements give similar results as Hamamatsu data sheets for the single pixel PMT R5600-00. For $\mathbf{B_X}$, the clear asymmetry between positive and negative values of the magnetic field is observed.

For the purpose of the AMS experiment, the maximum values of the magnetic field compatible with the signal reduction not exceeding 10-20% of the signal were calculated. These critical values of **B** ($\mathbf{B_{10\%}}$ and $\mathbf{B_{20\%}}$) were measured for several high voltages applied on the HV divider; the results are presented on figures 13, 14 and 15. One can observe a very slow variation of $\mathbf{B_{10\%}}$ and $\mathbf{B_{20\%}}$ for X, Y and Z components with HV (as expected, when increasing the HV, the PMT become slightly less sensitive to **B**). The values of $\mathbf{B_{10\%}}$ and $\mathbf{B_{20\%}}$ are summarized in table I :

Magnetic field (Gauss)	B_X	B_Y	B_Z
$B_{10\%}$	+12 -40	+70 -70	+12 -12
$B_{20\%}$	+20 -55	+100 -100	+17 -17

Table I: The values of the magnetic field corresponding to the signal reduction of 10% and 20%.

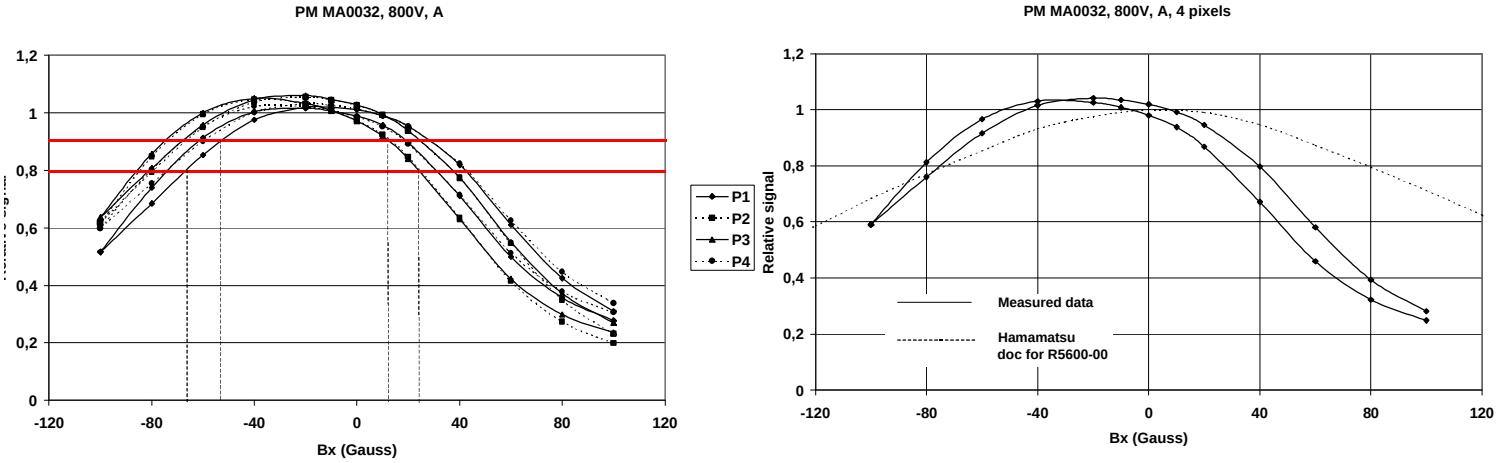

Figure 10. Left: Relative signal collected for 4 pixels of the photomultiplier as function of the magnetic field in the X direction. The two red lines correspond to 10% and 20% of the signal reduction. Right: Signal averaged over 4 pixels, compared with the dependence expected from Hamamatsu data sheet for single pixel, equivalent photomultiplier (R5600 type). Note the asymmetry between positive and negative magnetic field and small hysteresis of the signal.

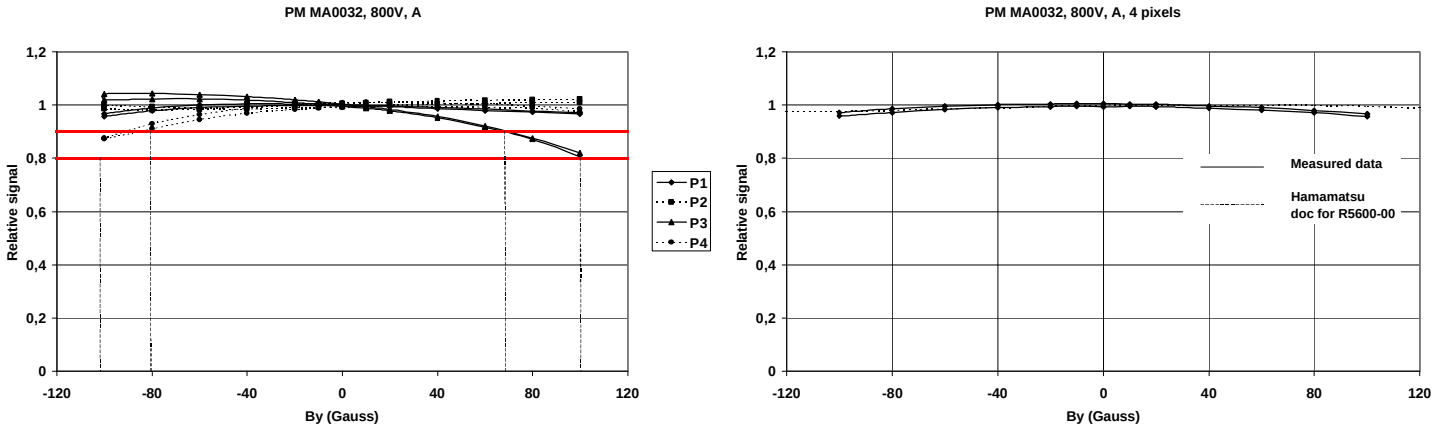

Figure 11. Same as figure 10, but for the magnetic field in the Y direction. The sensitivity of the photomultiplier is much smaller for magnetic field in Y direction.

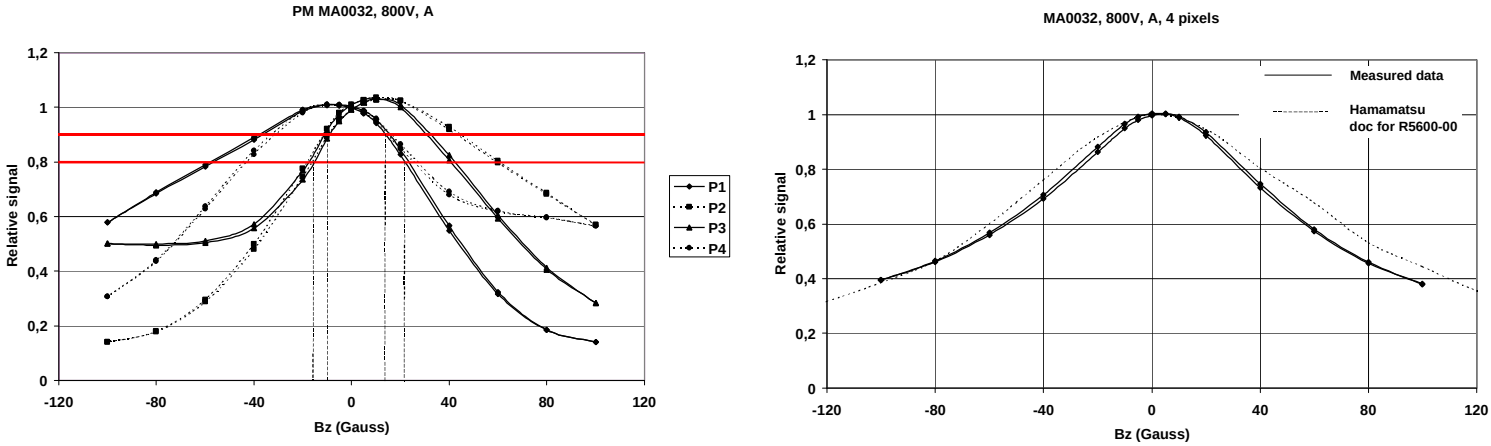

Figure 12. Same as figure 10, but for the magnetic field in the Z direction. The sensitivity of each pixel behave differently, but the average sensitivity is symmetric with respect to $B_Z = 0$.

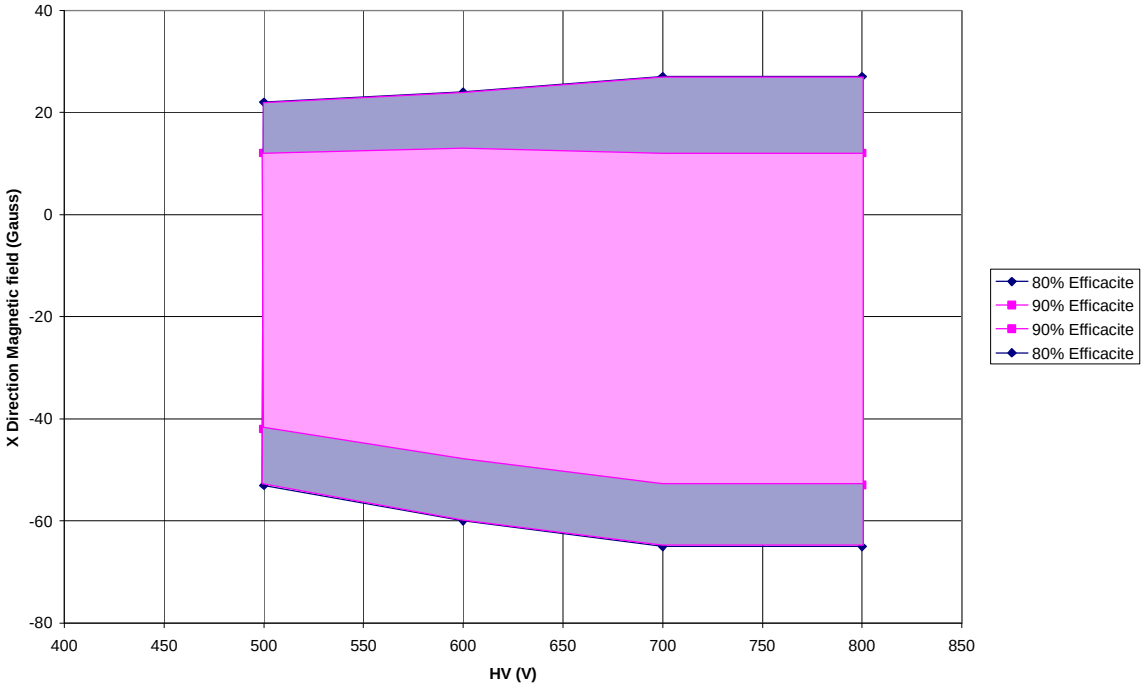

Figure 13. The values of the magnetic field applied in the X direction of the photomultiplier corresponding to 10% and 20% signal reduction as function of the high voltage applied on the divider. 10% signal reduction corresponds to the minimum magnetic field of +12 Gauss and –40 Gauss. For 20% reduction the corresponding values are +20 and –55 Gauss.

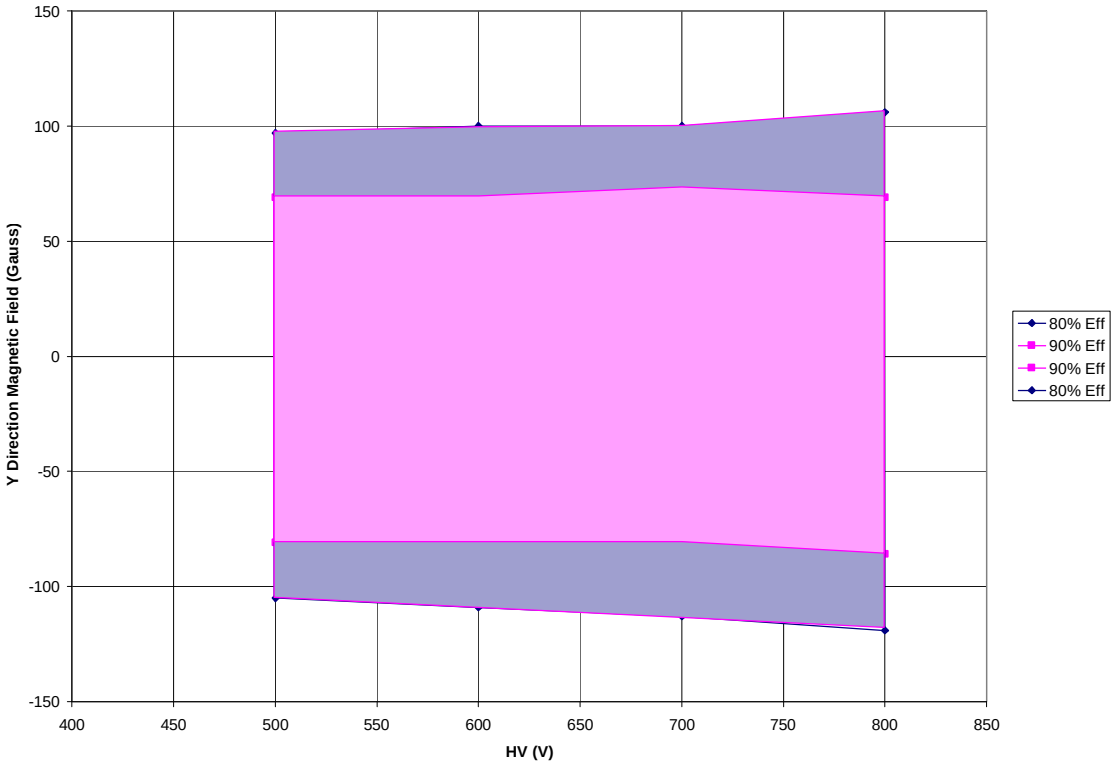

Figure 14. Same as figure 13, but for magnetic field in Y direction. The 10% signal reduction corresponds to minimum B_Y = ±70 Gauss, the 20% reduction for B_Y = ±100 Gauss.

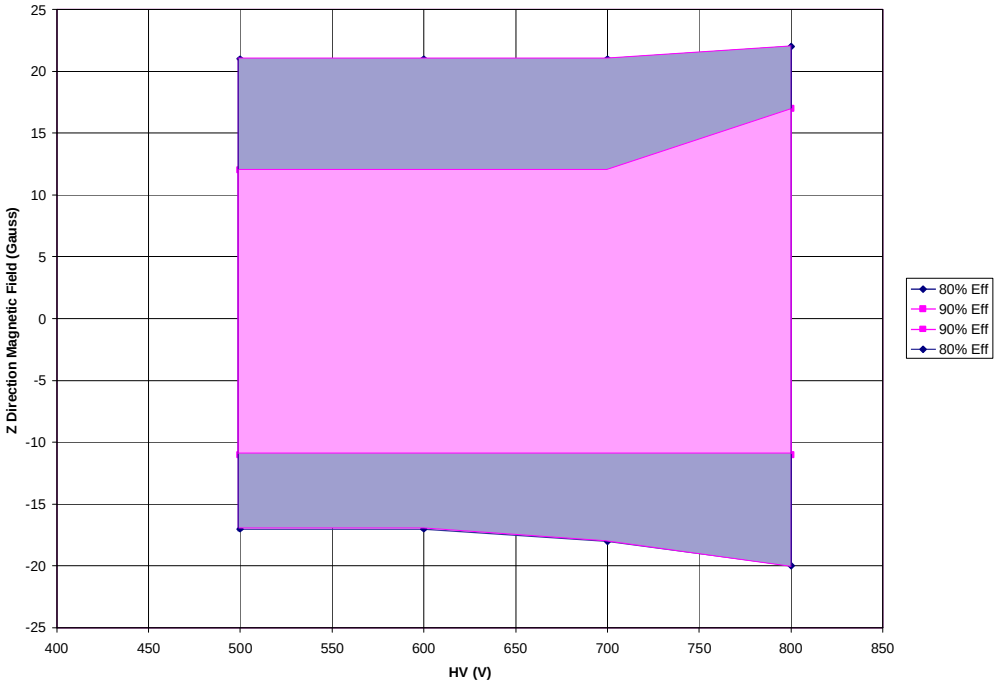

Figure 15. Same as figure 13, but for magnetic field in Z direction. The 10% signal reduction corresponds to minimum B_Y = ±12 Gauss, the 20% reduction for B_Y = ±17 Gauss.

3. Optimization of the dynamic range of the photomultiplier

As it was mentioned in the introduction, the main requirement for the photomultiplier used in the AMS-02 electromagnetic calorimeter is to support the high dynamic range of light pulses created by cosmic rays in the calorimeter fibers. In order to cover the maximum dynamic range, the optimization of the HV and of the HV dividers was necessary. The signal of the photomultiplier, corresponding to this optimum working point, was then used as input to conceive the dedicated front-end integrated circuit [6].

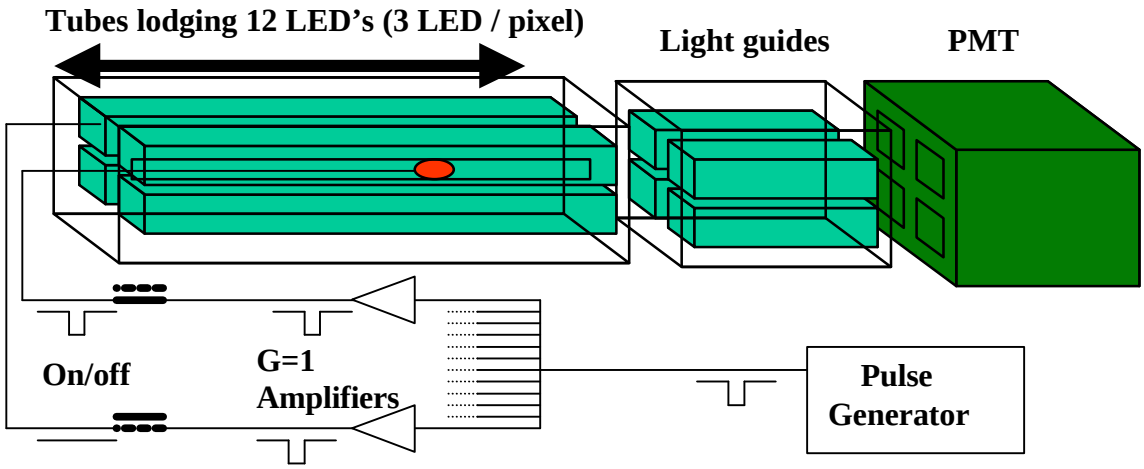

Figure 16: Schematic diagram of the experimental set-up used for the measurement of the dynamic range of the PMT.

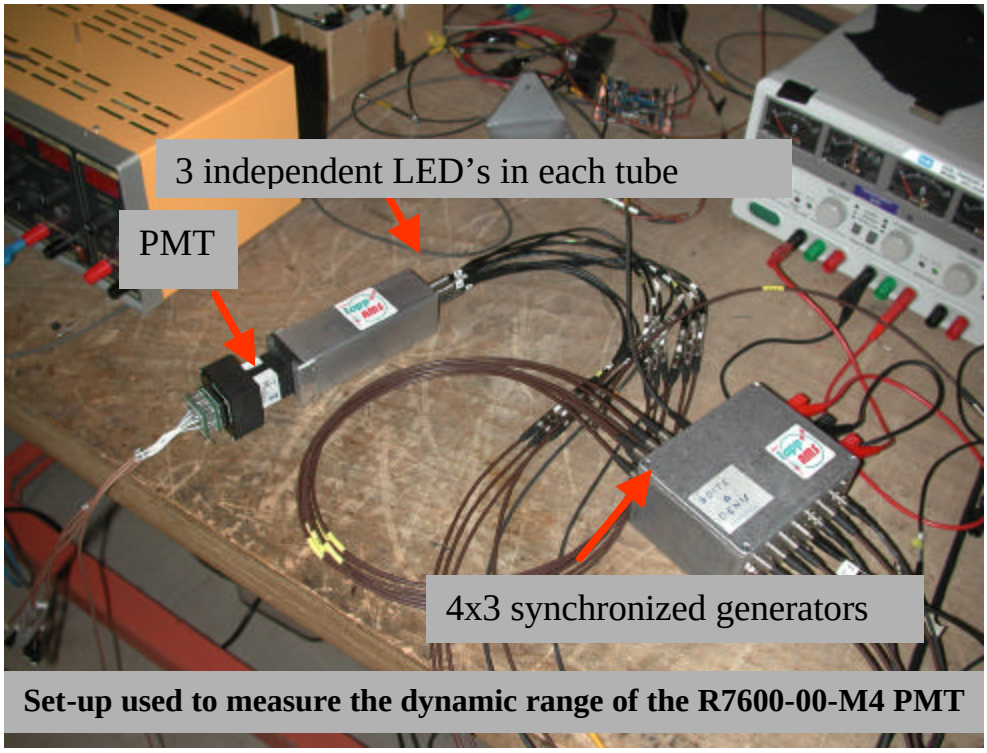

Figure 17: Experimental set-up used for the measurement of the dynamic range of the PMT.

The schematic drawing and the picture of the experimental set-up are presented in figures 16 and 17: 3 independent LED's were placed in front of each pixel of the PMT. All 12 LED's were supplied by the same generator followed by 12 independent buffers. This ensured, for a given LED, that the light signal was stable when connecting or disconnecting other LED's. The quantity of the light could be varied in the large range by displacing LED's inside the tubes and/or by varying the signal of the generator. Output signals of four pixels of the PMT were send to the charge integrating ADC through 50Ω cables.

The method used to detect the saturation point was the following: for a fixed LED position and fixed generator signal, the output signal of the PMT was collected for LED_1 ***ON*** and LED_2 ***OFF***, for LED_1 ***OFF*** and LED_2 ***ON*** and, finally, for LED_1 and LED_2 both ***ON***. From these 3 signals (S_1, S_2 and S_{1+2}) the following deviation from the linearity was then calculated:

$$g = \frac{S_{1+2} - (S_1 + S_2)}{S_1 + S_2}$$

For a given photomultiplier, given HV divider and given HV value, the value of ***g*** was calculated for different values of the output signals. Figure 18 shows a typical dependence of ***g*** as function of output signal of the PMT. One can observe a constant, close to zero value of ***g*** until about Q_{sat} = 2000 pC, and then a strong decrease, corresponding to the saturation of the PMT.

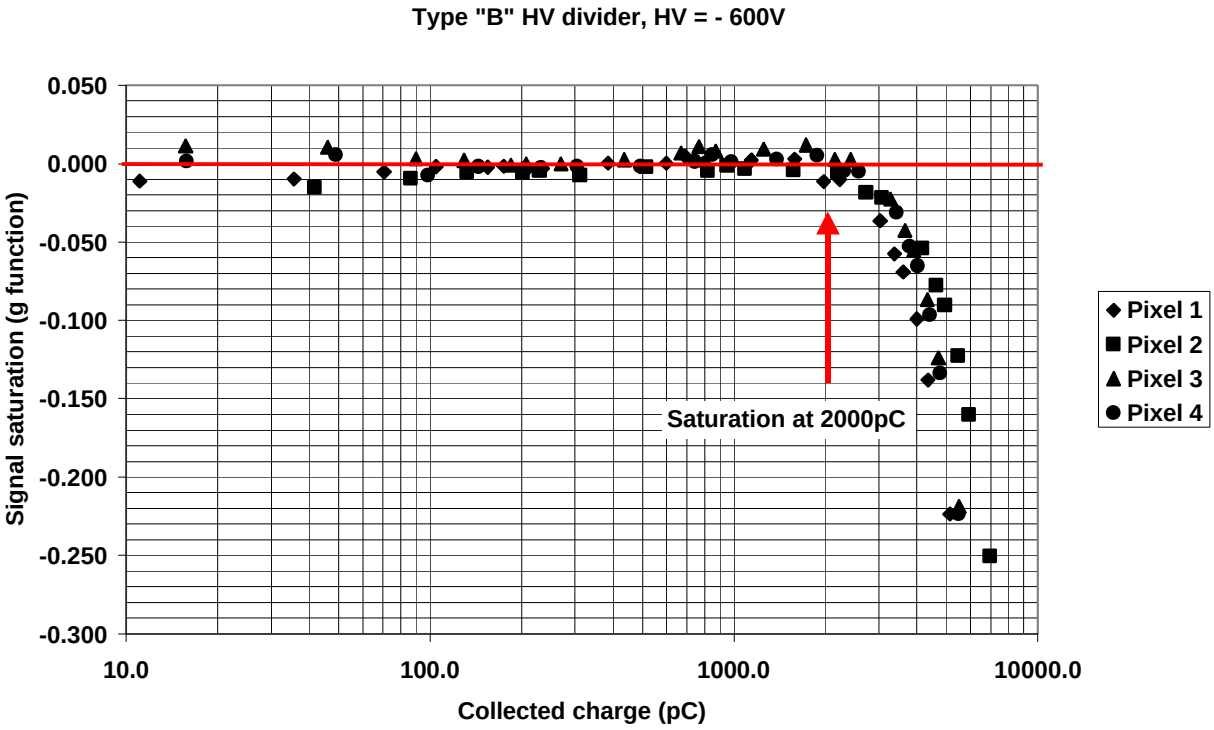

Figure 18: The saturation of the PMT response as function of collected charge (see text).

In parallel, the gain ***G*** of the photomultiplier was evaluated from the signal value and from the signal RMS by the method described in section 1. Finally the number of photoelectrons, corresponding to the saturation point was deduced:

$$Npe_{sat} = \frac{Q_{sat}}{eG}$$ where ***e*** is the charge of the electron.

The measurement was performed for 4 different HV dividers. The "standard" HV divider, proposed by Hamamatsu as "A" type, corresponds to the optimization of the single photoelectron resolution. Hamamatsu proposes the second «standard» HV divider, called «B» type as high dynamic range one. The third type, called "C", was suggested by Hamamatsu company as high dynamics and low voltage one. Finally the forth divider, called "D" corresponds to the one developed by Atlas group for electromagnetic calorimeter. The resistor chains for these four dividers are shown in table II and in figure 19:

	A		B		C		D	
	R(kΩ) (C(nF))	R/R_0	R(kΩ) (C(nF))	R/R_0	R(kΩ) (C(nF))	R/R_0	R(kΩ) (C(nF))	R/R_0
PhCath - D_1	330	1.5	330	1.5	660	3	470	2.5
$D_1 – D_2$	330	1.5	330	1.5	660	3	470	2.5
$D_2 – D_3$	330	1.5	330	1.5	660	3	200	2.5
$D_3 – D_4$	220	1	220	1	220	1	200	1
$D_4 – D_5$	220	1	220	1	220	1	200	1
$D_5 – D_6$	220	1	220	1	220	1	200	1
$D_6 – D_7$	220	1	220	1	220	1	200	1
$D_7 – D_8$	220	1	220	1	220	1	200	1
$D_8 – D_9$	220 (10)	1	220 (10)	1	220 (10)	1	200 (10)	1
$D_9 – D_{10}$	220 (10)	1	430 (10)	2	440 (10)	2	470 (10)	2.5
$D_{10} – P_{1,2,3,4}$	220 (10)	1	820 (10)	3.7	1100 (10)	5	470 (10)	2.5

Table II: The values of resistors and capacitors used in four studied HV dividers.

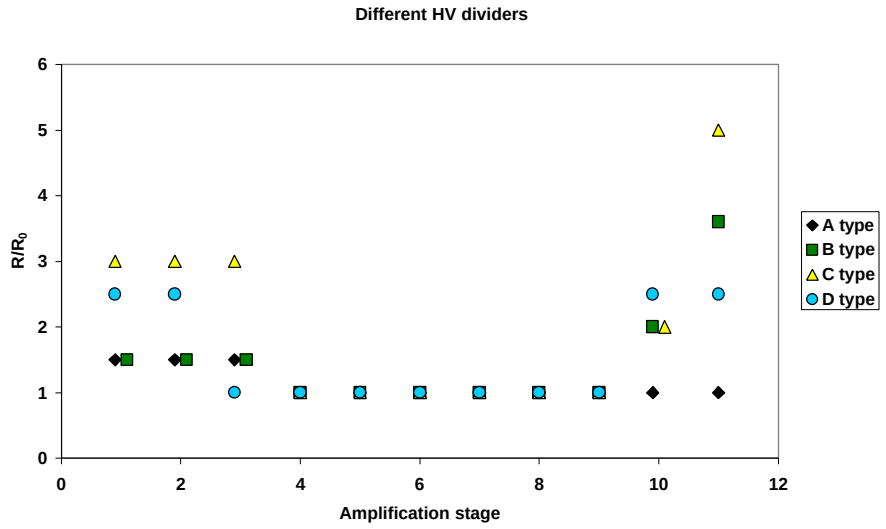

Figure 19: Relative values of resistor chains used in different HV dividers.

Table III summarizes the values of Q_{sat}, G and Npe_{sat} measured for 2 different PMT's and for different types of the HV dividers:

PMT n° 1 : serial number : 9J16C2

Type	HV (V)	400	500	550	600	700	800
A	Q_{sat} (pC)	200	300		400		900
	G	20000	100000		500000		6000000
	Npe_{sat}	62500	18800		5000		940
B	Q_{sat} (pC)	350	800		2000		2000
	G	10000	30000		140000		1300000
	Npe_{sat}	219000	167000		89000		9600
C	Q_{sat} (pC)		400	500	550		800
	G		10000	20000	40000		350000
	Npe_{sat}		250000	156000	86000		14000

PMT n° 2 : serial number : MA0032

Type	HV (V)	400	500	550	600	700	800
A	Q_{sat} (pC)				450		1000
	G				260000		3700000
	Npe_{sat}				11000		1700
B	Q_{sat} (pC)		500		1000	2000	2000
	G		12000		50000	180000	650000
	Npe_{sat}		260000		125000	69000	19000
D	Q_{sat} (pC)				1000		3000
	G				74000		730000
	Npe_{sat}				84000		26000

Table III: Values of Q_{sat}, G and Npe_{sat} measured for all studied systems.

The results from Table III are presented in figures 20 – 24. Figures 20, 21 and 22 show the evolution with the HV of Q_{sat}, G and Npe_{sat} for two different PMT's and the HV divider of B type and figure 23 - the relation between G and Npe_{sat} for this two different PMT's. As it can be observed in figure 23, for both PMT's the common relation allows to predict Npe_{sat} for a given G. As expected, Npe_{sat} decreases rapidly with G. Figure 24 shows the relation between G and Npe_{sat} for all studied HV dividers. For a given gain, the maximum of photoelectrons can be measured for the HV divider of B type. For this divider, for a gain of $5*10^4$, Npe_{sat} = 150000, it decreases to 120000 for $G=10^5$ and to 30000 for $G=5*10^5$. The maximum light signal expected in the calorimeter corresponds to 1 TeV electrons developing the electromagnetic shower and gives about 100000 photoelectrons [4]. From this consideration it is clear that the most appropriate HV divider is of B type and that the gain of the photomultiplier should not exceed 10^5.

The opposite part of the dynamic range corresponds to signals of the lowest amplitude to be measured. It corresponds to minimum ionizing particles (MIP) and represents about 8-9 photoelectrons [4]. It was necessary, before the final design of the front-end electronics, to measure the capability of the PMT to measure this low-level signal with B type HV divider and for the gain not exceeding 10^5. For this test the PMT was directly coupled (no cable) to the amplifier of 2kΩ entrance impedance. The output signal of the amplifier was then send to

the ADC via 50Ω cable. The result of the measurement is shown in figure 26. The spectra for HV ranging from 500 to 800 V (gain from 8 000 to 560 000) were collected for an LED signal corresponding to 8.5 photoelectrons (equivalent to MIP). As it can be observed in figure 26, the separation between this signal and the pedestal is satisfactory for HV not lower than 600V (gain $\geq 4*10^4$). It is shown in more quantitative way in figure 27, where the signal to background ratio is presented in function of the HV. For HV ≥ 600V the separation between the signal and the pedestal corresponds to the natural fluctuation of the Poisson distribution of 8.5 photoelectrons, whereas this separation deteriorates for lower HV.

The final parameters of the HV divider and the HV values, adopted by the AMS02 ECAL collaboration, are the following:

- HV divider of B type
- Gain of PMT of 10^5, corresponding to HV between 600V and 700V.

These parameters imply the front electronics to accept signals in the range from ¼ of the MIP (2 photoelectrons, e.g. 32 fC) to 1 TeV electrons (10^5 photoelectrons, e.g. 1.6 nC). Electronics group at LAPP [6] designs the dedicated integrated circuit, which fulfills these requirements.

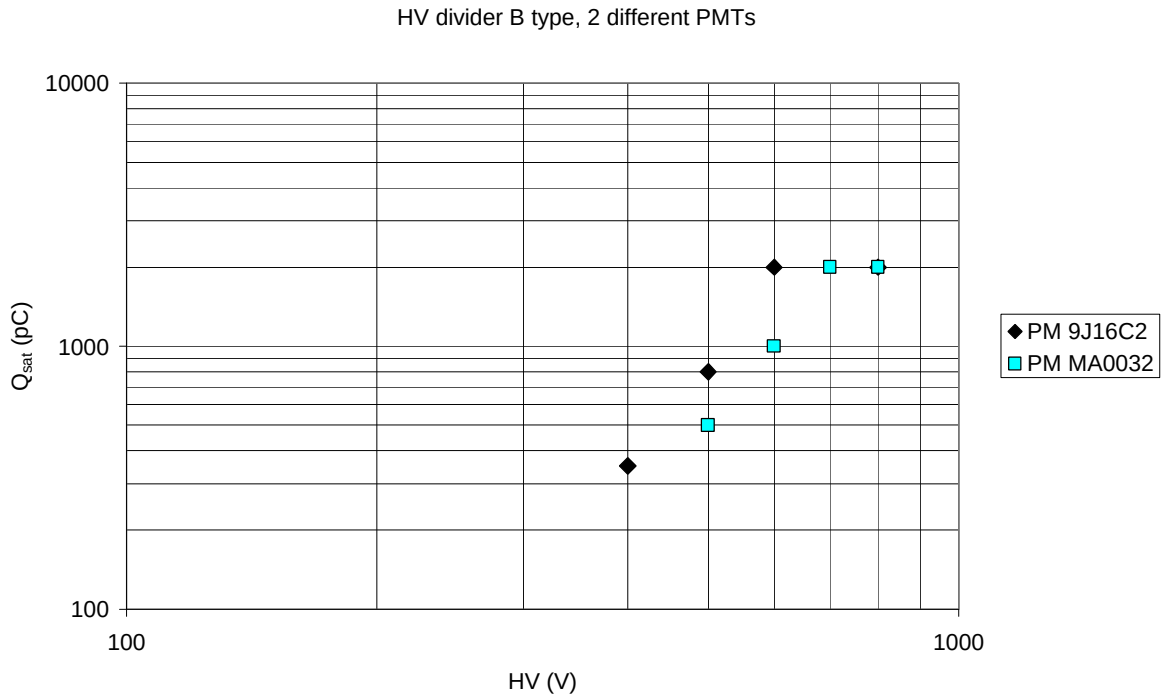

Figure 20: The variation of the charge corresponding to the signal saturation for two different PMT's as function of the HV. The HV divider was of "B" type.

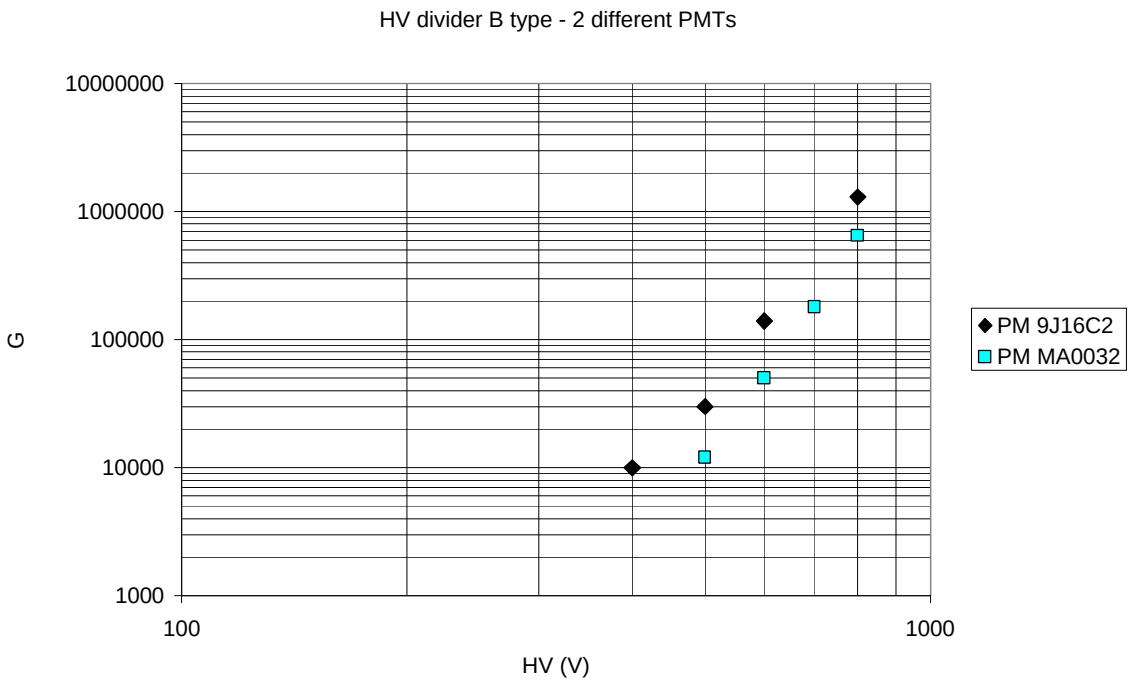

Figure 21: The variation of the gain for two different PMT's as function of the HV. The HV divider was of "B" type.

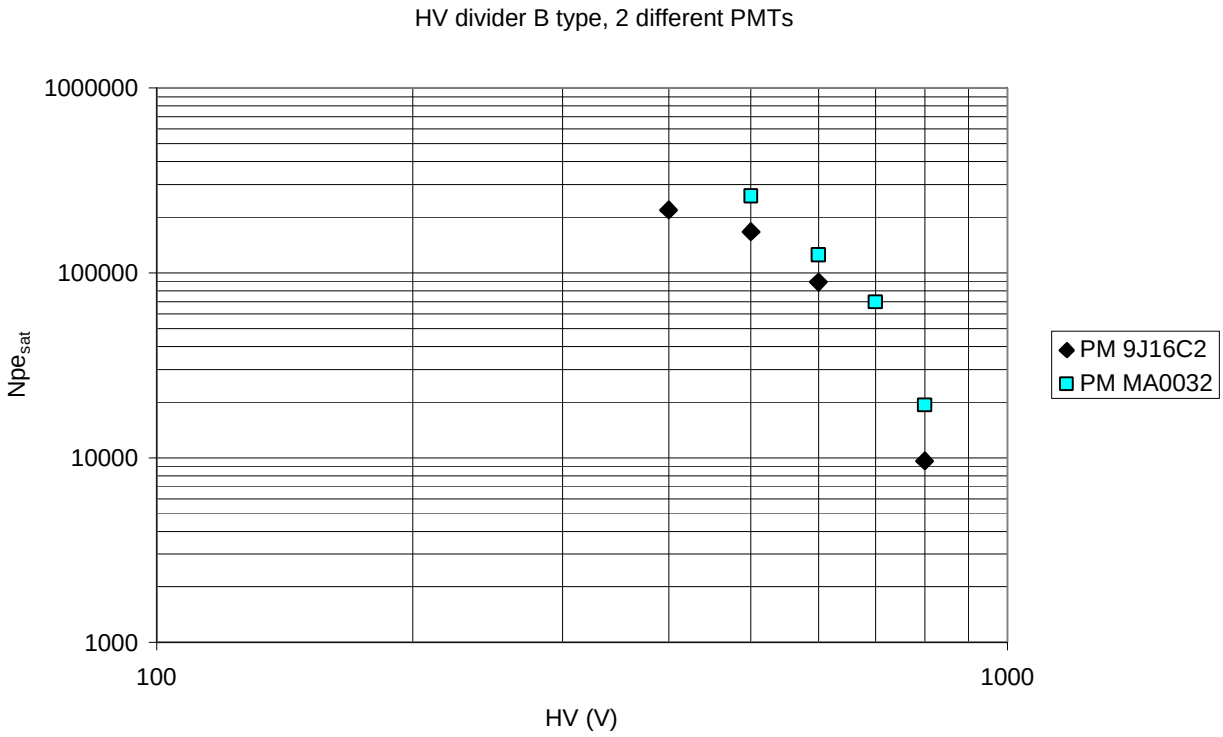

Figure 22: The variation of the number of photoelectrons corresponding to the saturation for two different PMT's as function of the HV. The HV divider was of "B" type.

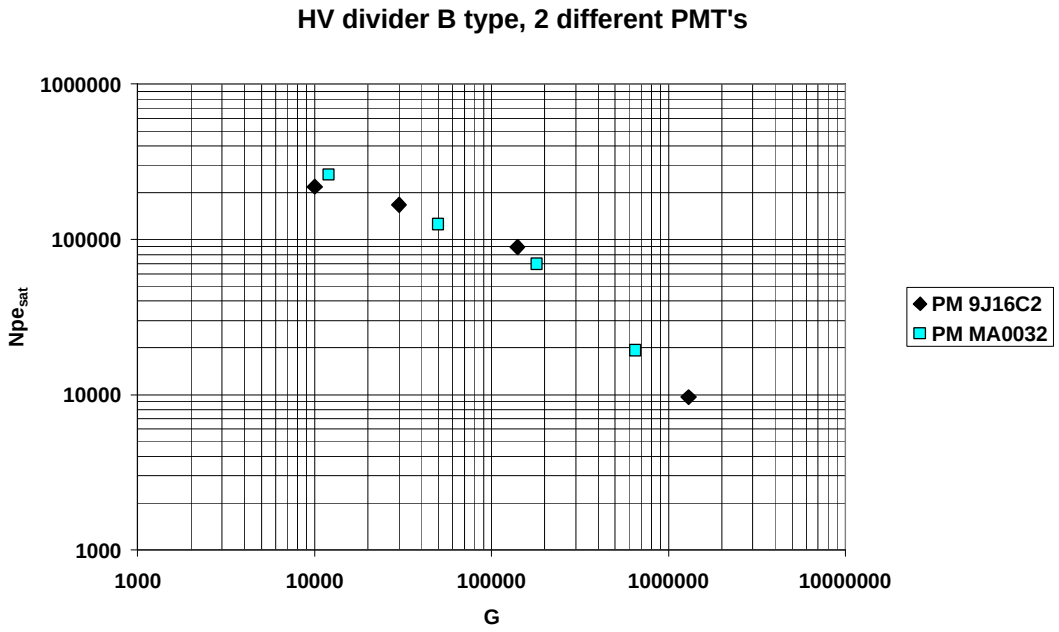

Figure 23: Relation between the number of photoelectrons at saturation point and the gain of the photomultiplier ("B" type HV divider).

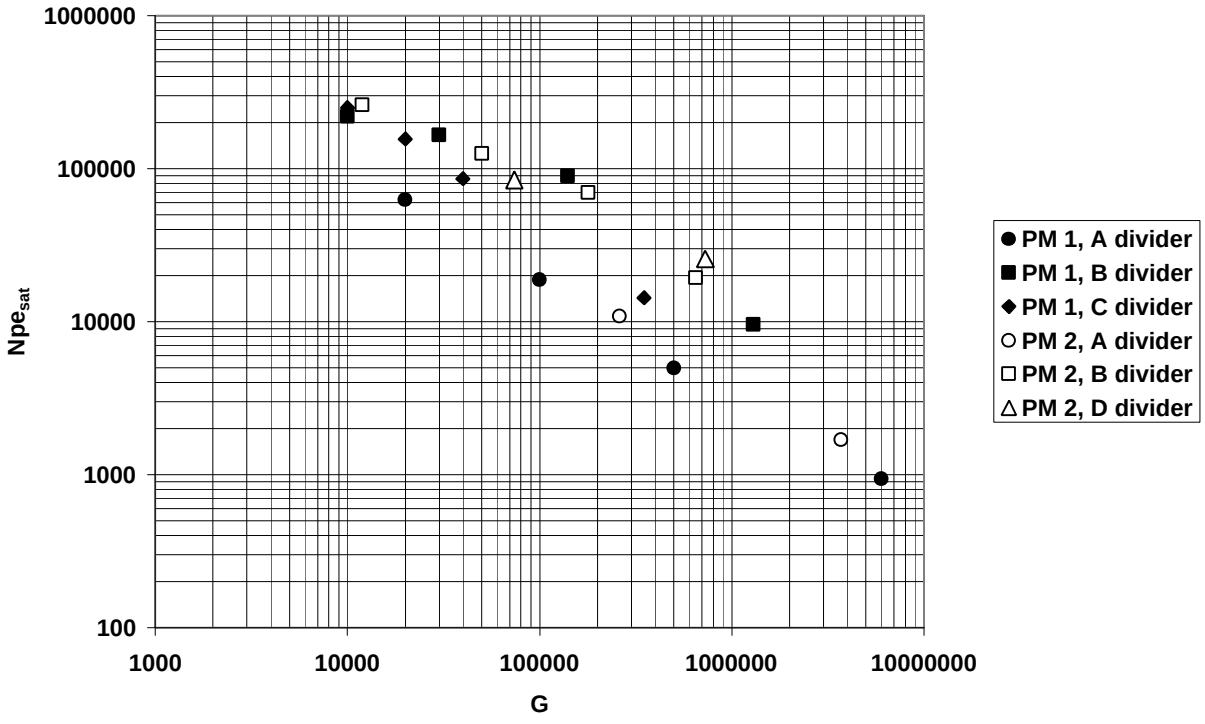

Figure 24: Relations between the number of photoelectrons at saturation point and the gain of the photomultiplier for different HV dividers.

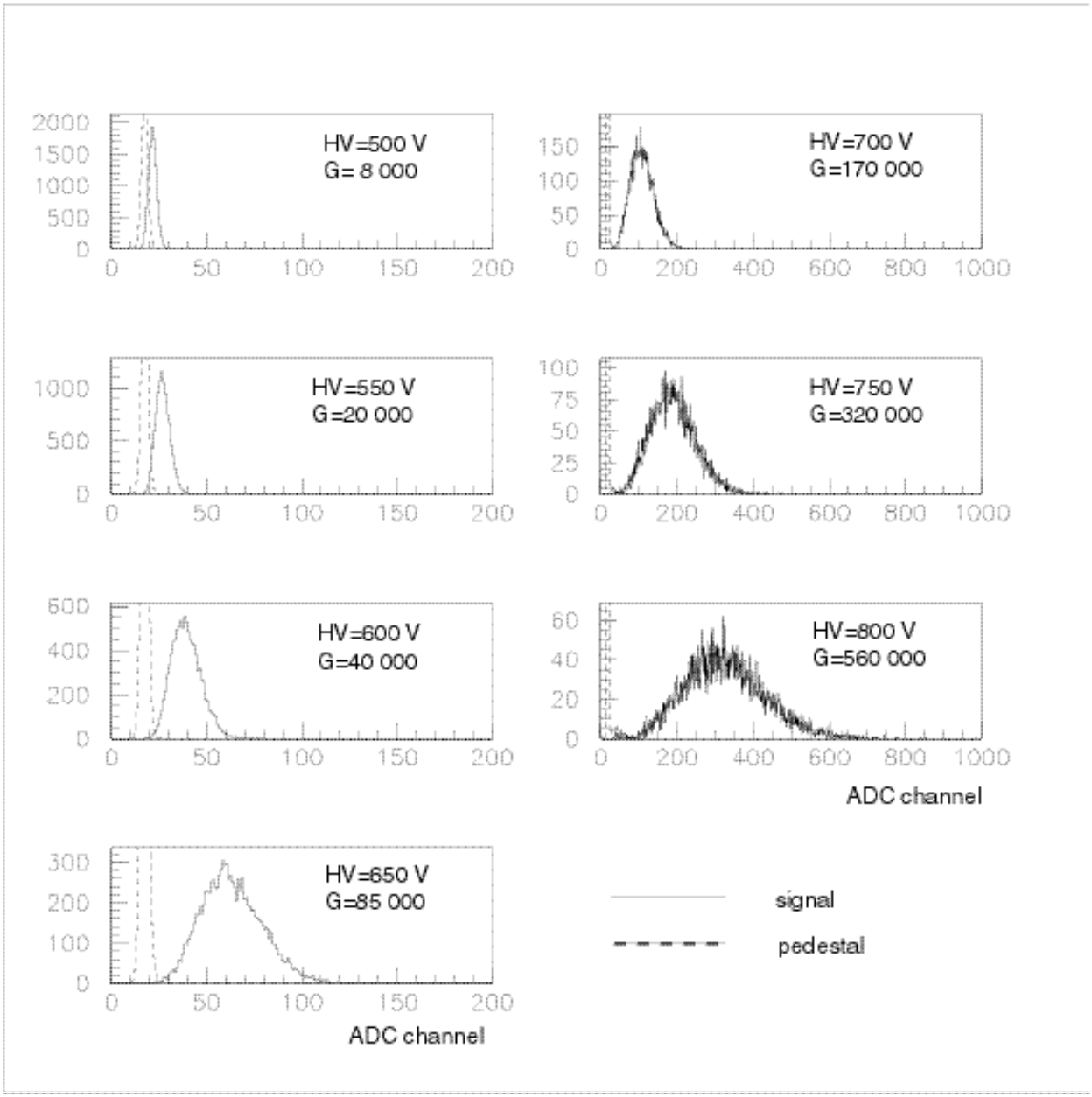

Figure 25: Spectra collected for 8.5 photoelectrons LED signal and pedestal at different HV ("B" type HV divider). The amplifier of 2kW input impedance was directly coupled to the HY divider of the photomultiplier.

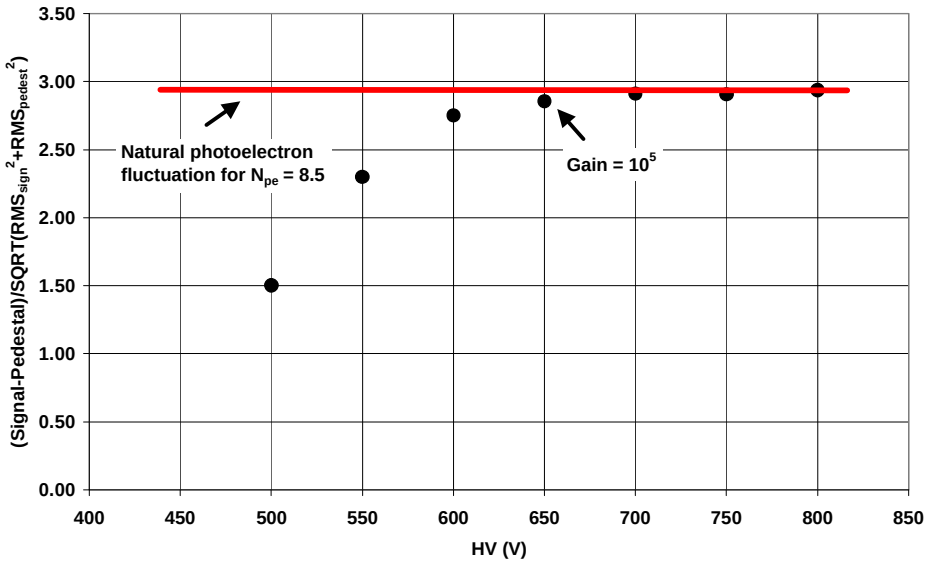

Figure 26: The separation of the signal and the pedestal as function of the HV. The natural fluctuation of the signal corresponding to 8.5 photoelectrons corresponds to RMS = 2.9.

Conclusions

The extensive study of the R7600-00-M4 photomultiplier from Hamamatsu was done with the aim to optimize its performances for the AMS02 electromagnetic calorimeter:

- the detailed scanning of the photocathode allowed optimizing dimensions of the light collecting cones: the maximum aperture without cross talk between pixels was adopted.
- the influence of the magnetic field was systematically measured. It gives the input to detailed calculations of the magnetic shielding of the PMT's.
- the dynamic range of the PMT was maximized by selecting the optimum HV divider and the optimum gain of the photomultiplier. These parameters gave input to the design of the dedicated front-end integrated chip.

Acknowledgement

Students who contributed to the measurements described in this paper: Jean Sebastien Roch and Peter Turba are acknowledged.

References

[1] http://ams.cern.ch/AMS/ams_homepage.html and references quoted there.
[2] B.Alpat – "AMS on ISS" – talk given on the Conference Frontiers Detectors for Frontier Physics – 8th Pisa Meeting on Advanced Detectors, May 2000.
[3] Hamamatsu data sheet, March 1997.
[4] Monte Carlo simulations with Geant 4 – AMS collaboration
[5] F.Cadoux, R.Kossakowski, J.P.Vialle - AMS Note 2001-05-01.
[6] V.Hermel – "EMC electronics status" – presentation on AMS Technical Interchange Meeting, CERN, Juin 2001.